J Exp Biol Advance Online Articles. First posted online on 8 January 2015 as doi:10.1242/jeb.114868
Access the most recent version at http://jeb.biologists.org/lookup/doi/10.1242/jeb.114868

Mechanical challenges to freshwater residency in sharks and rays

Adrian C. Gleiss[1,2*], Jean Potvin[3], James J. Keleher[1], Jeff M. Whitty[1], David L. Morgan[1], Jeremy A. Goldbogen[2]

[1]Freshwater Fish Group & Fish Health Unit, School of Veterinary & Life Sciences, Murdoch University, 90 South Street, Murdoch, Western Australia 6150, Australia
[2]Hopkins Marine Station, Stanford University, Pacific Grove, CA 93950, USA
[3]Department of Physics, Saint Louis University, St. Louis, MO, 63103, USA

*author for correspondence: agleiss@stanford.edu

Running head: Mechanical challenges to freshwater residency

Summary

Major transitions between marine and freshwater habitats are relatively infrequent, primarily as a result of major physiological and ecological challenges. Few species of cartilaginous fish have evolved to occupy freshwater habitats. Current thought suggests that the metabolic physiology of sharks has remained a barrier to the diversification of this taxon in freshwater ecosystems. Here we demonstrate that the physical properties of freshwater provide an additional constraint for this specious group to occupy freshwater systems. Using hydromechanical modelling, we show that occurrence in freshwater results in two- to three-fold increase in negative buoyancy for sharks and rays. This carries the energetic cost of lift production and results in buoyancy dependant mechanical power requirements of swimming and increase optimal swim speeds. The primary source of buoyancy, the lipid-rich liver, offers only limited compensation for increased negative buoyancy as a result of decreasing water density; maintaining the same submerged weight would involve increasing the liver volume by very large amounts, namely, 3 to 4 fold in scenarios where liver density is also reduced to currently observed minimal levels, and 8 fold without any changes in liver density. The first data on body density from two species of elasmobranch occurring in freshwater (bull shark *Carcharhinus leucas* and largetooth sawfish *Pristis pristis*) support this hypothesis, showing similar liver sizes as marine forms but lower liver densities, but the greatest negative buoyancies of any elasmobranch studied to date. Our data suggests that mechanical challenges associated with buoyancy control may have hampered the invasion of freshwater habitats in elasmobranchs, highlighting an additional key factor that may govern the predisposition of marine organism to successfully establish in freshwater habitats.

Keywords: Buoyancy, liver, tissue density, locomotion, lift, drag

Introduction

A wide range of physiological, ecological, and evolutionary processes determine the capacity of animals to invade and adapt to novel environments. For major transitions, such as those between aquatic and terrestrial or marine and fresh water environments, successful invasions are relatively infrequent in most plant and animal taxa except for tetrapods (Vermeij and Dudley, 2000). However, transitions from saltwater to freshwater habitats can facilitate radiation and speciation events, which in some systems manifest as rapid and repeated invasions worldwide (Lee and Bell, 1999). The Chondrichthyes have proven relatively unsuccessful at invading freshwater habitats despite their worldwide distribution in marine ecosystems. Of the >1000 species of the Elasmobranchii, only approximately 5% are thought to reside in freshwater (Ballantyne and Fraser, 2013; Martin, 2005). Moreover, most of these species only utilise freshwater habitats for part of their lifecycle. Explaining the mechanism behind this stark pattern in biogeography has received significant attention in the literature for the last half century (e.g. Ballantyne and Robinson, 2010; Ballantyne and Fraser, 2013; Pillans and Franklin, 2004; Thorson, 1962).

Current hypotheses suggest that metabolic organisation of elasmobranchs is responsible for their poor penetration into freshwater, resulting in metabolic costs associated with osmoregulation (Ballantyne and Robinson, 2010; Meloni et al., 2002). Whereas the difference in solute concentrations has a significant impact on the physiological biochemistry of elasmobranchs, the potential impact of the changing density of seawater and freshwater has not been adequately considered. Although the difference in density between seawater (SW ~1026 kg m^{-3} at 20C°) and freshwater (FW ~996 kg m^{-3}at 20C°) may seem trivial, it may nevertheless have significant ramifications for the buoyancy control of these animals. Animal tissue is generally denser than both SW and FW, so that marine animals without any

organ providing buoyancy would be heavily negatively buoyant (Alexander, 1990; Davenport, 1999; Pelster, 2009). Elasmobranchs utilise lipid-rich livers to increase the buoyant force relative to their mass (commonly referred to as static lift) (Baldridge Jr, 1970; Bone and Roberts, 1969; Corner et al., 1969). Due to the minor difference in density of liver tissue (900 -1000 kg m^{-3}) to that of marine waters (~1027 kg m^{-3}), large livers are required to provide necessary force to approach near neutral buoyancy. Indeed, neutrally buoyant sharks, which are commonly found in the deep sea may have livers which comprise 30% of whole body volume (Corner et al., 1969) compared to only 1-7% swim-bladder volume required to provide neutral buoyancy in ray-finned fishes(Alexander, 1966; Davenport, 1999; Weitkamp, 2008).

Despite the use of the liver as a means to increase buoyancy, the majority of elasmobranch species remain negatively buoyant (Baldridge Jr, 1970; Bone and Roberts, 1969; Gleiss et al., 2011b). Counteracting this negative buoyancy represents one of the two major forces that govern the energetics of locomotion in aquatic environments (Alexander, 1990; Alexander, 2003). In elasmobranchs, the heterocercal caudal fin and the pectoral fins and/or the body generate vertical forces that balance this negative buoyancy (Fish and Shannahan, 2000; Wilga and Lauder, 2002). This in turn results in drag due to lift by the body and pectoral fins (known as induced drag, Alexander, 1990; Alexander, 2003) and the vortex jet of the heterocercal caudal fin to have a vertical component (Wilga and Lauder, 2002) making excessive negative buoyancy unfavourable. The use of a buoyancy organ, such as a large lipid rich liver, reduces this cost, but increases parasite drag, due to greater surface area and reduced streamlining (Alexander, 1990). Negative buoyancy is favourable for those animals travelling fast while neutral buoyancy provided by large livers favours lower travel speeds, as a result of decreasing costs of lift production at higher speeds (Alexander, 1990). For

instance, Greenland sharks (*Somniosus microcephalus*) have substantial liver sizes and are close to neutral buoyancy cruise at speeds of only 0.1 lengths/s (Watanabe et al., 2012). In contrast, sharks that are more negatively buoyant tend to travel at 0.2-0.7 lengths/s (Watanabe et al., 2012).

The close relationship between the locomotor performance and body density may represent a fundamental influence on the lifestyle of elasmobranchs (Bone and Roberts, 1969; Gleiss et al., 2011a) and a key aspect to understanding how the constraints of water density and buoyancy shape the lives of those species that occur in freshwater. However, this has received no attention in the literature thus far (Ballantyne and Robinson, 2010). In this paper, we aim to clarify the impacts of changing water density on the buoyancy and energetics of elasmobranchs. We model the expected change in buoyancy by calculating the theoretical buoyancies of marine species of shark occurring in freshwater. We then simulate the required change in liver size and density to compensate for the decrease in environmental density and calculate the energetic costs associated with different hypothetical scenarios of compensation. In a second part of this work, we present the first measurements of buoyancy of two species of elasmobranchs naturally occurring in freshwater and compare those to marine forms.

Results

Modelling the Morphological Implications of Water Density

Changes in water density drastically alter the submerged weight of an elasmobranch, in this case our modelled bull shark (Fig. 1), as calculated by eq. 1 described in *Materials and Method*. Submerged weight increases linearly with a decline of water density. A reduction of liver density to the low values observed in deep-sea sharks (920 kg m^{-3}) can off-set this increase to brackish waters of density of 1022 kg m^{-3} (Fig. 1). An additional mode of

compensating for the reduced environmental density is to change the size of the liver, with larger livers providing more upthrust. Assuming no adjustments in liver density, liver volume would have to increase 8-fold to maintain a similar submerged weight in freshwater as in marine waters (Fig. 1), resulting in a liver comprising ~60% of whole body volume. In the hypothetical scenario where a shark has the ability to reduce its liver density, liver volume would only have to increase 3-fold, resulting in a liver comprising ~35% of body volume, compared to 14% in marine waters to achieve the same submerged weight as in marine waters. We have to note here that these calculations assume that all other tissues maintain the same volume. This assumption is discussed below.

Fig. 1

Modelling the Energetic Consequences of Salinity

Negative buoyancy compensation via lift production by the body, pectoral fins and heterocercal tail, and attendant metabolic costs, was carried out using a standard approach to aircraft performance modelling - see eqns. 2 – 6a in *Materials and Methods* (Cole 1981, Pope 1951). Components of this model were validated with the shear stress drag data of smooth dogfish (*Mustelus canis*) measured by Anderson et al (2001) (further discussed in the Electronic Supplement). Swimming performance is assessed herein with the expended metabolic power (P_{total}) and Cost of Transport (COT) incurred from (parasite) drag production and from negative buoyancy compensation via lift (see eqns. 6a and 7). Herein these metabolic costs are based on two representative swim speeds, namely, the so-called *minimum speed* (u_{min}) used to minimize total drag (eqn. 5); and the optimal speed (u_{opt}) maximizing travel distance with a fixed energy store (Weihs, 1973). Teleosts and elasmobranchs also travel over long distance in manners to reduce energy consumption. But biological organisms incur metabolic costs at $u = 0$ (known as Standard Metabolic Rate)

resulting from the other energy intensive functions of the body; this cost demands that metabolic efficiency is achieved at higher velocities than u_{min} – hence the larger u_{opt}. Typically, sharks swim at average speeds in the range of 0.3 - 0.8m/s (Watanabe et al 2012) - presumably near optimal speed – which amounts to twice (or less) the minimal speed (as shown further here). Not surprisingly, both minimal and optimal speeds, and corresponding metabolic costs, increase with larger negative buoyancies (see eqns. 6a and 6b). This trend will be shown quantitatively here using u_{min} since it can be assessed with a minimum of assumptions. Given that the calculation of u_{opt} involves several inputs characteristic of metabolism, which predictably vary between species and encountered temperature, the dependence of optimal speed and metabolic expenditures shall be shown algebraically rather than numerically (see eqn. 6b below, and eqns. ES13-ES20 in the Electronic Supplement). Note finally that other optimized swimming speed concepts have been proposed (e.g. Castro-Santos, 2006; Videler and Nolet, 1990; Ware, 1978). Although optimizing different metrics, most, if not all, should show similar trends with regards to adding more negative buoyancy, due to the increasing mechanical cost associated with a given speed.

We simulated four hypothetical scenarios that could be a response to changing water density; no compensation, increasing liver size, decreasing liver density and the two combined. These four scenarios markedly differed in the parameters used in our modelling exercise (Table 1) and resulted in an increase of negative buoyancy compared to marine waters. The scenarios do not encompass all possible morphological adaptations, such as body and fin profiles to improve lift (of which an evolution into a ray-like lifting body profile would be one example). They aim instead at evaluating the effects of liver density and size modifications separately from those leading specifically to lift enhancement. Although the latter wasn't considered here, it should be clear from the modelling that, despite possible

reductions in parasitic drag, lift increase always come at a cost, either in extra induced drag and/or loss of turn rate performance in unsteady manoeuvring. All scenarios resulted in an increase of negative buoyancy compared to marine waters. We found a marked increase of the speed at which drag is minimised, primarily as a result of the increased negative buoyancy of those scenarios (Fig. 2).

An increase in liver size and a decreasing liver density resulted in the smallest increase of either cost of transport or metabolic power at minimum cost speed (u_{min}), but also resulted in less streamlining, with lower body depth over body length ratio (t/SL) and body wetted area both increased by 13% (Fig. 3). Our numerical work to solve u_{opt} also showed that optimal speed is dependent on buoyancy and mechanical power requirements increase with increasing negative buoyancy (see Methods and Electronic Supplement). Namely, both u_{opt} and P_{total} increase with negative buoyancy (W) as $u_{opt} \propto W^0$ & $u_{opt} \propto W^{1/2}$ at small and large negative buoyancy respectively, which, interestingly, compares with u_{min} as $u_{\min} \propto W^{1/2}$ (eqn. 5); and $P_{total}^{opt} \propto W^2$ & $P_{total}^{opt} \propto W$ again at small and large W.

Table 1

Fig. 2, 3

Densities of freshwater elasmobranchs

All sawfish (n=17) and bull sharks (n= 5) captured in the Fitzroy River were negatively buoyant in the water they were captured in, with calculated body densities of 1065 ± 5 kg m^{-3} for the bull sharks and 1065 ± 3 kg m^{-3} for the sawfish. The ratio of W_{sub} and weight in air W_{Air} (Mass x 9.81 m/s^2) was 6.44 ± 0.39% in bull sharks and 6.48 ± 0.33% in sawfish. For the individuals where liver size and density could be measured, the liver represented 6.21 ±

225 0.64 % of whole body mass in the sawfish (n=2) and 7.82 ± 1.73 % in the bull shark (n=3).
226 Liver density was 980 ± 2 kg m^{-3} in the sawfish and 920 ± 3 kg m^{-3} in the bull sharks (Table
227 3).
228
229 *Comparative Data*
230 Comparisons of the ratio between weight in air and submerged weight shows that the 22
231 individuals of the two species we studied show some of the greatest negative buoyancies (6.4
232 %), compared to the 113 individuals sampled in other studies in marine waters (3.95 ±1.2 %,
233 see supplementary Table ES1). Our statistical model of mass and submerged weight supports
234 this, with the most parsimonious model indicating that habitat and mass are the strongest
235 predictors of submerged weight (Table 4, Fig. 4). The comparison of liver size scaling
236 between elasmobranchs sampled in marine waters from previous research and those sampled
237 in freshwater revealed that there was little difference in the size of livers, with the highest
238 ranked model only including logMass as an explanatory factor. Lifestyle did not appear to
239 affect liver size in our data-set; this however is a result of excluding deep-water sharks from
240 our analysis, which are known to have large livers (Bone and Roberts, 1969; Corner et al.,
241 1969). Liver density on the other hand is best predicted by the inclusion of lifestyle and
242 habitat. Pelagic sharks have livers of lesser density than those species that are generally
243 associated with the seabed. The five individuals for which livers could be sampled showed
244 liver densities that were below or near the lower 95th percentile of individuals of similar
245 lifestyle sampled in marine waters (Fig. 4). Density of lean tissue was not predicted well by
246 any of the covariates we tested the model for (Table 4).
247
248 **Table 4**
249 **Fig. 4**

Discussion

Our comparison of body composition of sharks sampled in marine waters and those in freshwater suggest that liver size has not drastically increased to produce more upthrust and compensate for the lower density of freshwater. Liver density on the other hand was measured to be close to the lowest values observed in any species of shark, suggesting that this may be a response to reduced water density. We emphasize, however, that these conclusions do not stem from experimental data of how liver size and density responded to changing salinity in a controlled experiment, but rather a large comparative analysis of liver sizes and densities of a range of species. We can, however, safely say that no substantial increase in liver size appears to have occurred in the individuals we studied. The same caveat also applies to our assessment of liver density; however in this case, the liver densities were lower than the 95th percentile of those studied to date, indicating that liver density may be readily lowered. There is precedence for such a process in the literature – experimentally weighted spiny dogfish (*Squalus acanthias)* increase their fraction of DAGE (a low density lipid) in liver tissue (Malins and Barone, 1970). Although not explicitly quantified in their study, greater amount of DAGE will increase the upthrust provided by the liver and compensate for the increased negative buoyancy. No change in liver size was found in the experimentally weighted spiny dogfish.

Our analysis makes one important assumption; we have assumed that all lean tissue is fixed in its volume. A reduction in the volume of dense tissue (e.g. muscle, viscera, skeleton), would reduce any increases in surface area and therefore the energetic consequences we outline here. However, any reduction in the volume of these tissues must invariably decrease some form of performance. For instance, a reduction of white muscle volume (the most

voluminous tissue in most fish) would be expected to lead to a proportional decline in burst swimming performance. A simple example, for a shark to maintain similar hydrodynamic characteristics (fineness ratio, buoyancy, wetted area, Table 1) the liver would have to occupy ~45% of the whole fish, reducing lean tissue volume by >50% in freshwater. Assuming white muscle comprises 70-40% of the animals volume (Bone, 1978; Greek-Walker and Pull, 1975), this would result in a 76 - 100% reduction in available white muscle for burst swimming, with obvious deleterious effects to fitness (Ghalambor et al., 2003; Walker et al., 2005). Even though it may be possible to maintain similar hydrodynamic properties, compensation by reduction of volume of other tissue should have additional deleterious effects.

Optimal compensation – a paradox?

Our field data indicate that the reduction of liver density is the prevalent mechanism by which sharks achieve more upthrust. Yet our modelling approach suggests that in addition to decreasing liver density, increasing liver size to 30% body volume (Scenario 4) provides a more efficient alternative in our hypothetical shark (see Fig. 2), due to the reduced negative buoyancy. However, increasing liver size will increase body fineness ratio (t/SL), and thus wetted area (by ~13%), as well as parasitic drag force (by >25%, see eqn. 2, 3); but interestingly it would also *decrease* u_{min} (by ~ 18%; see eqn. 5) and overall COT (Figure 2) compared to the scenario lacking compensation. However, less streamlining by increased liver volume would also degrade the performance of burst swimming as well as of foraging at supra-optimal speeds [44] since, with $u > u_{min}$, the resulting drag force would become even higher and to the point of *increasing* COT, perhaps at levels too high for the given fixed amount of muscle power and energy available. In other words, combining lower liver

299 densities with larger liver volumes could only be advantageous in environments where the
300 prey is easy to find and catch (at u_{min}) and predation pressure is low.
301
302 An additional explanation for this discrepancy is the metabolic cost of growing and
303 maintaining such large livers. The low-density lipids contained in the liver responsible for
304 providing upthrust are energy dense. For instance, triacylglycerols, a class of lipid found in
305 shark livers (Wetherbee and Nichols, 2000), contains 38 kJ g^{-1} whereas muscle tissue
306 contains approximately 2-4 kJ g^{-1}. This may make a substantial difference for the juvenile
307 sharks studied here, which are in a period of rapid somatic growth. Indeed, Priede et al.
308 (2006) have suggested that the metabolic cost associated with large livers may be responsible
309 for the absence of sharks from the oligotrophic abyssal depths of the oceans. Moreover, liver
310 tissue has some of the fastest turnover time of any tissue in elasmobranchs (Hussey et al.,
311 2010), therefore increasing the cost of not only growing but also maintaining such tissue.
312 Although it may be argued that ~30% liver volume is encountered in deep-sea sharks and
313 some very large pelagics (e.g. basking, tiger or white sharks) and is therefore unlikely to
314 provide an overwhelming metabolic burden, the warm tropical waters occupied by our study
315 subjects already significantly increase standard metabolic rates (Carlson and Parsons, 1999).
316 The increasing metabolic cost of growing a large liver may therefore not be sustainable for
317 juvenile elasmobranchs in tropical waters.
318
319 *Ecological Implications*
320 Activity represents an important component of the energy balance of most fish (Boisclair and
321 Leggett, 1989) and our results indicate that greater negative buoyancies will result in
322 increased costs, as shown by our modelled increases in u_{min} and u_{opt}. Such behavioural
323 modification will increase the energetic cost of locomotion because such power costs increase

with swimming speed at exponents of 2-3 (Alexander, 2003; Lowe, 2001). Our results confirmed that despite some compensation by liver density, the negative buoyancies of the two species we studied are approximately twice as great as those of a typical marine elasmobranch of similar mass and lifestyle. At u_{min} the power required to swim is approximately doubled compared to marine water. At u_{opt}, on the other hand, the power would be expected to increase by as much, if not more, depending on the value of GW^2/β. The increased activity costs will depend on a variety of species-specific factors including the ecology of the species, typical swimming speeds, and the amount of time spent resting on the bottom.

Evolutionary Implications

Increasing costs of locomotion associated with freshwater residency itself does not preclude elasmobranchs from occupying freshwater habitats, but it may act as a constraint. Teleost fish often compete for the same ecological space with elasmobranchs, but the utility of a gas bladder as a source of upthrust largely negates the buoyancy problem faced by sharks and rays. Juvenile coho salmon (*Oncorhynchus kisutch*) collected along a salinity gradient display compensation in swim-bladder volume; in marine waters a bladder comprising 5% of whole body volume is adequate to provide near neutral buoyancy and in freshwater this volume only increases to 7% (Weitkamp, 2008). This difference is unlikely to affect parasite drag, as surface area and fineness ratio will remain largely unchanged (Alexander, 1966). Indeed, the extraordinarily low density of air (~ 5 kg m^{-3} at 10 m depth at 25 C°) compared to that of lipid (~900 kg m^{-3}), results in water density not having a great effect on upthrust provided in fish using gas filled bladders. This suggests that elasmobranchs (and by extension all fish that utilise lipid only to provide upthrust) are disadvantaged in freshwater over those using gas.

Paleontological records also show that early elasmobranchs were not always scarce in freshwater, but dominated marine and freshwater environments by the late Devonian, ~400 million years ago, whereas ray-finned fishes only evolved into efficient swimmers in the Mesozoic, approximately 200 million years ago (Long, 1995). We therefore argue that the innovations by modern teleosts, the gas-bladder and its role in buoyancy control in particular, have resulted in a competitive edge over elamsobranchs and contributed to the contemporary low abundance and diversity of freshwater sharks and rays. The material constraints of tissues providing lift in elasmobranchs will inevitably result in greater negative buoyancies in freshwater and result in lower locomotory performance compared to those groups able to use gas. This effect can be somewhat offset, however, it appears that sharks are unable to escape the constraints of lipid-produced upthrust.

The patterns of diversity in freshwater elasmobranchs also supports our conclusions; ~76 - 84% of all elasmobranchs known to occupy freshwater are part of the order Myliobatiformes (Ballantyne and Fraser, 2013; Martin, 2005). Myliobatiforms are a group of largely benthic rays, such as whiprays (*Himantura* spp.) and stingrays (*Dasyatis* spp.). Individuals within this group are largely confined to movement close the substratum (with some exceptions) and often occur over flat sandy or muddy substrates. The costs of increased negative buoyancy would be drastically reduced in those species, due to benthic resting and the majority of swimming being performed close to the substrate. Swimming close to the bottom reduces the induced drag by a lifting surface as a result of increased pressure forming on the ventral side of the lifting surface, known as the ground effect (Webb, 1988). Indeed, in gliding bird flight, the ground effect may be responsible for a 49% reduction of drag due to lift (Hainsworth,

1988). The generally higher density of liver tissue in benthic elasmobranchs supports this, as there is less of an energetic incentive to reduce submerged weight in this group.

Our paper is the first to demonstrate that the reduced density of freshwater represents a significant physical challenge for elasmobranch locomotion that manifests as greatly increased negative buoyancy. These results indicate that freshwater sharks partially compensate with lower density liver tissue, rather than increasing overall liver volume. Given these data, elasmobranchs in freshwater habitats experience significant negative buoyancy and can only compensate by generating more lift through forward locomotion. Such behavioural compensation will result in greater energy expenditure from increased drag and we argue that buoyancy may have been an important factor constraining the reinvasion of freshwater by sharks and their relatives that may act in concert with osmoregulatory challenges. Additional data on the organismal biology of elasmobranchs occupying salinity gradients as well as paleontological records will be necessary to test these competing, but not mutually exclusive hypotheses.

Methods

Modelling the morphological consequences of environmental density

The following section largely follows the arguments by Alexander (Alexander, 1990), who tested the optimal means of producing lift as a function of swimming speed. Our model is constrained to a single means of producing increased buoyant force (liver lipid), while considering the implications of changing density of the occupied medium. The primary source of increasing the buoyant force in elasmobranchs is the liver, which is characteristic of lower density (~900 - 1000 kg m^{-3}) than other tissues of a shark (~1070 kg m^{-3}), the ratio of

liver-tissue to non-liver tissue is a major determinant of the buoyancy of a shark. According to Archimedes,

$$W = ((V_{Lean}\,\rho_{Lean} + V_{Liver}\,\rho_{Liver}) - (V_{Lean} + V_{Liver})\ \rho_{Water}\ )\,g \qquad \text{eqn. 1}$$

where W refers to the submerged weight (or negative buoyancy) and *g* to the acceleration of gravity (9.81 m/s^2). Moreover, V_{Lean} and V_{Liver} are the volume of lean and liver tissue respectively and ρ_{Lean} and ρ_{Liver} are their respective densities. Thus the overall volume and density of the shark are given by $V_{Shark} = V_{Lean} + V_{Liver}$ and $\rho_{Shark} = (V_{Lean}\,\rho_{Lean} + V_{Liver}\,\rho_{Liver})/V_{shark}$, respectively.

Here we define lean tissue to be all tissue excluding the liver. This set of equations in turn permits us to estimate the physical consequences of changing water density, i.e. changing ρ_{Water} to 996 kg m^{-3}, representing the density of freshwater at 28 °C compared to 1026 kg m^{-3} of marine water on submerged weight and the liver size required to off-set the reduced upthrust provided by the environment. These two phenomena were also investigated under the assumption that sharks could alter the density of their livers, which has been experimentally shown for *Squalus acanthias* (Malins and Barone, 1970). A low value for liver density was taken to be 920 kg m^{-3}, representing the livers of deep-sea sharks (Bone and Roberts, 1969; Corner et al., 1969) as these animals must face similar constraints in reducing their submerged weight, while presumably minimizing liver size.

Modelling the energetic consequences of changing water density

We investigated, from first principles, the energetic consequences of a hypothetical shark moving into freshwater, and considered a range of mechanisms that could be employed to compensate for the decreasing water density as compared to the marine conditions. Changing

buoyancy impacts the attendant metabolic expenditures given the changes in swimming speed, as well as in body lift and drag, which are required to maintain a level trajectory. Such changes are being assessed herein with the type of aerodynamic modelling that is common in aircraft design (Dole, 1981; Pope, 1951). The basics of this modelling, along with the most important results will be discussed in this section, and the mathematical details further explored in the Appendix and Electronic Supplement (ES1).

Although the inclusion of low-density lipids in the liver reduces negative buoyancy, hydrostatic forces are not sufficient to achieve neutral buoyancy in most species. In elasmobranchs (and many other obligate swimmers) this is achieved through forward motion-generated lift, which in turns increases drag. Swimmers face two general (physical) energetic costs incurred by moving through their environment, namely, those related to *parasite* drag ($F_D^{parasite}$), as generated by the fluid's friction against the body, as well as from the low pressure of the wake turbulence behind the body; and to *induced* drag ($F_D^{induced}$), as created by the lift production arising from the upward-angling of the anterior portion of the body and pectoral fins, and also from the downward thrust component created by the asymmetric caudal tail. For leopard shark (*Triakis semifasciata*) the balance of lift production is estimated at approximately 45% from the pectoral fins and 55% from the caudal fin (Fish and Shannahan, 2000), and we note that these values represent the only force balance estimates for dynamic equilibrium in sharks.

Parasite drag applied to a shark moving at speed *u* can be generally calculated as

$$F_D^{parasite} = \frac{1}{2}\rho_{water} u^2 \cdot SA \cdot C_D^{parasite} \qquad \text{eqn. 2}$$

Here SA is the reference surface area used when extracting the parasite drag coefficient ($C_D^{parasite}$) from experimental data (usually, by inverting eqn. 2). In comparative biomechanics SA is the body wetted area, approximated here as two joined paraboloids, namely SA = 0.71(girth x pre-caudal length), as further discussed in the Electronic Supplement (ES1, eqn. ES.5). On the other hand, the parasite drag coefficient is modelled as the sum of the parasite drag (i.e., friction plus pressure drag) arising separately from the body and from all fins: $C_D^{parasite} = C_D^{parasite}|_{body} + \sum C_D^{parasite}|_{fins}$ ("$\sum$" symbolizes a sum over each fin's contribution). The body parasite drag ($C_D^{parasite}|_{body}$) is expressed in a form developed by Hoerner in his drag studies of bodies of revolution (Blevins, 1992) :

$$C_D^{parasite}\Big|_{body} = \frac{K}{\mathrm{Re}^{\alpha}}\left[1 + 1.5\left(\frac{t}{SL}\right)^{3/2} + 7.0\left(\frac{t}{SL}\right)^{3}\right] \qquad \text{eqn. 3}$$

The parasite drag due to all fins can be expressed similarly, albeit in a more complicated form, and is further discussed in the Appendix and Electronic Supplement (ES 1, see eqns. A.1.and A.2; and ES.6, ES.8 and ES.9). Here the effects of *pressure* drag are represented by the terms in *t/SL*, with *t* representing the body's maximum diameter without the fins and *SL* the pre-caudal length. The coefficient K/Re^{α} represents the effects of the fluid's shear stress on the body, with Re as the body's Reynolds number, $Re = SL \cdot u/\nu$, and with ν as the fluid's kinematic viscosity (1.15×10^{-6} and 1.13×10^{-6} m^2/s for sea water and fresh water (16 ^oC) respectively)). The fins' parasite drag coefficient likewise includes a similar friction factor. The coefficient *K* and exponent α (>0) parameterize the fluid's friction as the combined result of a shark's denticulated skin and swimming motions on the body (Oeffner and Lauder, 2012; Shelton et al., 2014). Recent studies of shark hydrodynamics make it clear that the

interactions of the boundary layer generated by the skin's denticles interacts with the flows created by the tail's motions in ways that do not always minimize body drag, and moreover in ways that are difficult to quantify in simple formulas such as in eqn. 3 (Shelton et al., 2014). In the interest of simplicity, the values of K and α correspond to those of a smooth flat plate in longitudinal flow and supporting a turbulent boundary layer (K = 0.072 and α = 0.2 (Blevins, 1992)). It should be stressed that using flat plate drag data should not be viewed as approximating shark skin as smooth; but rather, as a proxy for translating the complex interactions between denticulated skin and tail motions, as suggested by the averaging of the few rigid body and active swimming drag data so far available on a single shark species (Anderson et al., 2001).

The total drag exerted on the body is calculated by adding induced drag to the parasite drag of eqn. 2. The former is derived from the fact that the induced drag coefficient is proportional to the square of the lift force (Dole, 1981) and is given by

$$F_D^{induced} = \frac{(1+\delta)}{\pi AR} \cdot \frac{(F_{lift})^2}{\left(\frac{1}{2}\rho_{water} u^2\right) \cdot LS \cdot WD} \qquad \text{eqn. 4}$$

Parameter AR is an overall body aspect ratio, here defined as that of the body's maximum width, plus combined pectoral fin span, over pre-caudal body length SL (or $AR = WD/SL$). The force F_{lift} is the total lift generated by *all parts of the body*. Since it is assumed that the shark is swimming horizontally and at constant speed, lift thus equals negative buoyancy ($F_{lift} = W$). Finally, δ is an aerodynamic efficiency factor that is set to zero [14] (with aircraft, δ is typically less than 0.05).

Estimation of the metabolic expenditures connected to increased drag-production involves a metric of speed. Postponing the study of expenditures generated at the optimal speed (Weihs,

494 1973), we first consider metabolic expenditures incurred at speeds $u = u_{min}$ where total drag is
495 *minimal* (Alexander 1990). As discussed further in (Dole, 1981), a point of minimum drag
496 exists in cases where lift equals weight in aircraft (or body lift equals negative buoyancy in
497 sharks), as parasite and induced drag are proportional to u^2 and $1/u^2$ respectively.
498 Furthermore, u_{min} is also the point at which *induced drag is equal to parasite drag*. Thus
499 solving the latter constraint with equation eqn. 2 and 4 yields a way to calculate u_{min}:
500

501 $$(u_{\min})^4 = \frac{1}{\frac{1}{2}\rho_{water} \cdot WD \cdot LS \cdot C_D{}^{parasite}} \cdot \frac{2W^2}{\pi (WD)^2 \rho_{water}} \qquad \text{eqn. 5}$$

502

503 Note that from eqns. 3, A.1 and A2 (and ES.7 and ES.8), it follows that $C_D{}^{parasite}$ is also
504 proportional to $(1/u_{min})^{\alpha}$, with α defined by eqn. 3, so that the final dependence on negative
505 buoyancy will be as $u_{min} \sim W^{1/(4-\alpha)}$ (or $\sim W^{1/3.8}$ using the flat plate proxy). This result, used
506 along with eqn. 2, thus suggest that increasing negative buoyancy will indeed lead to higher
507 swim speed and thus to higher drag.
508
509 The total metabolic power (P_{Total}) required for a shark to move its body through the water at
510 u_{min} will be given by:

511 $$P_{total} = \frac{1.5F_D{}^{total}}{\eta} u_{\min} = \frac{1.5F_{thrust}\cos\theta}{\eta} u_{\min} \qquad \text{eqn. 6a}$$

512

513 The second equation highlights the fact that the thrust has a vertical component due to the lift
514 produced by the heterocercal caudal fin. In cases where the latter ~ *0.55W* (Fish and
515 Shannahan, 2000) the thrust's angle θ with respect to the horizontal would be calculated from
516 $\tan\theta = 0.55W/F_D{}^{total}$. The factor 1.5x arises from those effects of lateral tail-beat undulations

(which increase the required thrust) that remained unaccounted for by the proxy factor $K/Re^{0.2}$ above (this proxy averages friction drag of rigid and swimming scup and dogfish in Anderson et al. (Anderson et al., 2001)). (In comparison, a factor of 2.5 – 3 fold has been used in fish as compared to a rigid model (Webb, 1971b)). Finally, the factor η measures both metabolic and propulsive inefficiencies of the tail and body, and set here to $\eta \sim 0.20$ (Webb, 1971a).

Being oriented perpendicularly to a shark's motion at all times means that the lift force used to compensate for negative buoyancy does not perform any mechanical work on the body. However, lift generation *does* involve metabolic energy production since lift production *always* incurs additional drag in comparison to an identical body generating no lift. This can be done by re-writing P_{total} as resulting from the power used to compensate for *total* drag, i.e., from the sum of parasite drag (eqn. 2) and induced drag (eqn. 4). As discussed further in the Electronic Supplement (ES1), and evaluated for any arbitrary speeds u, one has:

$$P_{total} = \frac{1}{\eta_{sw}} \left[\left(\frac{1}{2} \rho_{water} \cdot SA \cdot {C_D}^{parasite} u^3 \right) + \frac{(1+\delta)}{\pi (WD/SL)} \frac{2W^2}{\rho_{water} (WD \cdot SL) \cdot u} \right] + W_m \qquad \text{eqn. 6b}$$

Here η_{sw} is a speed-dependent function ($\eta_{sw} = \beta u$) representing both metabolic and propulsive efficiency of the tail's propulsive apparatus, and the constant W_m the Standard Metabolic Rate corresponding to the internal metabolic processes that are independent of speed during active swimming (Weihs 1973). The second term in eqn. 6b is what distinguishes a fish swimming horizontally while neutrally buoyant ($C_L = 0$), and an elasmobranch doing the same but at C_L

539 $\neq 0$. With the latter and at minimum speed, this second term shows an explicit dependence
540 on, and an increase with, negative buoyancy (~ W^2).
541
542 The increased metabolic cost of swimming at the optimal speed (u_{opt}) while experiencing
543 increased negative buoyancy can be assessed by using eqn. 6b along with the approach
544 proposed by Weihs (1973). This is done by optimizing the distance travelled (l) at fixed
545 stored energy ($E = P_{total}\, l/u$), i.e., as a solution of the differential equation $dl/du|_{opt} = 0$ under
546 the constraint of lift-compensated negative buoyancy. As shown in the Electronic
547 Supplement (ES1) P_{total} would increase with negative buoyancy (W) as
548 $P_{total}^{\ opt} = 2W_m + 4GW^2/\beta u_{opt}^{\ 2}$ with $G \equiv 2(1+\delta)/(\pi AR \cdot \rho_{water} \cdot SL \cdot WD)$. The optimal speed increases
549 with W as well, namely as $u_{opt} \propto W^0$ & $u_{opt} \propto W^{1/2}$ at small and large negative buoyancy
550 respectively, after solving the algebraic equation $3GW^2/\beta = \left(\tau/\beta\, u_{opt}^{\ 4} - u_{opt}^{\ 2} W_m\right)$ where
551 $\tau \equiv \frac{1}{2}\rho_{water} S A C_D^{\ parasite}$. Here the parameter GW^2/β determines the regime where the negative
552 buoyancy can be considered as "small" or "large". Using typical shark morphological inputs,
553 this ratio is estimated at ~ 0.3 – 0.6 *Watts* m^2 s^{-2}, which places sharks somewhere in between
554 the two limits. With both β and W_m being unknown in sharks, a quantitative assessment of the
555 increased costs associated with higher negative buoyancy is currently out of reach.
556
557
558 Equations 2-6a,b and ES 14 now allow us to calculate a power-velocity relationship , i.e.,
559 where velocity = u_{min} and = u_{opt} respectively for hypothetical sharks in water of different
560 densities. It has to be noted, that these equations are not analogous to the metabolic rate-
561 swimming speed relationships (where u is an independent variable), but rather are designed to
562 provide the lowest hypothetical costs of swimming at a given water density even though no

563 single shark can have an ideal pectoral fin (or body angling) to maximise lift-to-drag ratio
564 over the range of speeds simulated. Indeed, some species will feature morphological
565 adaptations for faster cruising whereas others for slower speeds. We have also reflected this
566 in our efficiency term η, which would be expected to vary with swimming speed of an
567 individual, but here we will assume that the muscle geometry and tail-beat kinematics are so
568 that η is maximised at u_{min}, mimicking a fish adapted to the cruising speed that minimises
569 required power. Muscular efficiency has been experimentally determined for rainbow trout
570 (*Onchorhynchus mykiss*) and showed that maximum efficiency achieved was 20% (Webb,
571 1971a).
572
573 Finally, to facilitate comparisons of the energetic impact of changing water density, we
574 computed the net cost of transport (COT_{net}) to reflect the energetic cost of moving the animal
575 (and its variable mass depending on liver size) 1 m in distance.
576

577 $$COT_{net} = \frac{P_{total}}{u_{\min} m} \qquad \text{eqn. 7}$$

578
579 With regards to the drag calculations, the necessary input morphometric data for the bull
580 shark and smooth dogfish discussed in the sections below are listed in Tables ES1 – ES4.
581
582 We decided to model 4 hypothetical scenarios (see Table 1 for all parameters used in the
583 models described previously) that sharks could use to counteract changing buoyancies*:*
584
585 *Scenario 1 – No compensation*

586 Elasmobranchs do not alter their morphology in response to changing environmental density
587 and the mechanical costs of swimming change in accordance with the increasing negative
588 buoyancy.
589
590 *Scenario 2 – Reduced Liver Density*
591 Elasmobranchs have been shown to respond to experimentally increased negative buoyancy
592 by decreasing the density of their livers (Malins and Barone, 1970), effectively increasing the
593 buoyant force and reducing negative buoyancy. This scenario would result in no change in
594 liver size (and no changes in surface area), but would dampen the increase in negative
595 buoyancy with decreasing water density. We consider a liver density of 920 kg m^{-3} to be a
596 lower bound of liver density. Livers of this density are encountered in neutrally buoyant
597 sharks such as *Cetorhinus maximus* (Bone and Roberts, 1969).
598
599 *Scenario 3 –Increasing Liver Size*
600 Increasing the size of the liver is another mechanism by which more upthrust can be
601 generated and the impact of decreasing water density can be mitigated. We consider that 30%
602 of the body volume to comprise of liver tissue to be the upper ceiling of hypothetical livers.
603 This represents a realistic upper bound. Similar liver sizes are encountered in sharks that are
604 close to neutral buoyancy and these species face a similar constraint in minimising negative
605 buoyancy. Increasing liver volume while maintaining the volume of lean tissue is expected to
606 increase surface area and decrease fineness ratio, affecting parasite drag.
607
608 *Scenario 4 – Increasing Liver Size and reduction of Liver Density*
609 This scenario represents a combination of scenarios 2 and 4. The two distinct processes can
610 act synergistically in providing more buoyancy. We modelled the energetic consequences of

these four scenarios, using the observed body composition of bull sharks (*Carcharhinus leucas*) captured in Florida by Baldridge (1970). Namely, we consider that the lean tissue density is 1075 kg m^{-3}, the nominal liver density is 964 kg m^{-3} and liver volume represents 11% of whole body volume. We parameterised this model with a shark of 1m pre-caudal length and an associated mass of 15 kg (Thorburn, 2006).

Field Methods

Capturing of animals

Largetooth sawfish (*Pristis pristis*) and bull sharks were captured between September and October 2011 and 2012 in the Fitzroy River, Western Australia. Animals were captured using bottom-set gill-nets (15 and 20 cm stretched mesh-size) set at night. Nets were checked at regular intervals of 1.5 hours.

Measurement and calculation of body density

Captured sawfish and bull sharks were initially sexed and measured. Animals were weighed to the nearest 5 g using a sling and digital hanging-scale (UWE HS 7500 series, Capacity: 7500g, Resolution: 5g). To determine the submerged weight (W_{sub}) of the animals, a sling was suspended from a tripod (Daiwa infinity weigh tripod) in water of approximately 1.2 m depth. Before animals were placed into the sling, the weight of the sling was zeroed. Animals remained motionless in the sling and a weight was read after the scale stabilised. While weighing, it was ensured that no part of the sling touched the river-bed or the tripod. After submerged weight was determined, we measured the mass of animals using the same sling and scale, without submergence. Care was taken that no water remained in the sling when the mass was determined. Following these measurements, whole body density (ρ_{Shark}) was calculated based on the density of freshwater at 28 °C, the common water temperature during

night time (Gleiss & Morgan, unpubl. data) with a corresponding water density of 996 kg m^{-3}, as determined by the relation $\rho_{shark} = (W_{air}\ \rho_{water})/(W_{air} - W_{sub})$.

Determination of Liver density and liver-free body density

All individuals that perished in gill-nets were used for further analysis of buoyancy regulation. After determining whole body density, fish were dissected and liver density and volume was determined by displacing livers in a graded water cylinder. Livers were forcefully submerged with a long toothpick, to overcome positive buoyancy. The volume of the toothpick was negligible in relation to liver volume. Liver density (ρ_{liver}) was simply calculated from mass and displaced volume. Density of the liver-free body (ρ_{lean}) was determined in the same fashion as prior to dissection of the liver, by determination of mass and submerged weight using the described sling.

Meta-analysis of densities in marine and freshwater elasmobranchs

In order to compare buoyancy between marine and freshwater forms, we collated all such measurements from the literature, primarily based on two publications (Baldridge Jr, 1970; Bone and Roberts, 1969). Some parameters were not reported in these original papers (e.g. liver-free density), but could be calculated based on the data provided. We excluded any deep-sea individuals from the analysis due to significantly different densities (near neutral) as a result of the different lifestyle, as well as the basking shark for the same reason, resulting in 113 Individuals of 27 marine species being included in the analysis. In order to compare our data from freshwater elasmobranchs to the marine forms, we analysed the data using Mixed Models, due to unbalanced sample size for the different species (Zuur et al., 2007). To account for these repeated measures on a single species, we used the species ID as a random effect in our model. Models also included lifestyle as a covariate, which was determined

based on the species description in Compagno (2001), separating species into two groups considered to exclusively associate with the sea-bed (demersal), and those that swim in the water-column (pelagic & bentho-pelagic, see Supplementary Table ES1), as previous papers have shown the impact of lifestyle on buoyancy in elasmobranchs (Bone and Roberts, 1969). Mixed Models were fitted using the" lme4" package implemented in the R statistical package (R Development Core Team, 2010) and model selection was based on small sample corrected Akaike's Information Criterion (AIC_c) computed in the model selection package "MuMin".

Appendix. The parasite drag of fins

An aircraft wing's drag is calculated with computer programs that, from an airfoil's known shape and dimension data, yield the parasite and induced drag, the lift force and aerodynamic moments. Having no information about the airfoil profiles of shark fins, we resort to an approach similar to that of eqn. 3. Here again the parasite drag of airfoils and fins generate both friction and pressure drag, with the latter being generally much smaller than the former. The effects of both on each fin is represented by another equation developed by Hoerner, but applied to symmetrical airfoils ((Blevins, 1992); p. 352):

$$C_D{}^{parasite}\Big|_{fin} = C_{friction}{}^{fin}\left[1 + 2.0\left(\left\langle\frac{t_{fin}}{FC}\right\rangle\right) + 60.0\left(\left\langle\frac{t_{fin}}{FC}\right\rangle\right)^4\right] \qquad \text{eqn. A.1}$$

The pressure drag terms in $\langle t_{fin}/FC\rangle$ represent the mean *fin maximum thickness over fin chord*, as averaged over chord span. Herein $\langle t_{fin}/FC\rangle = 0.2$ *for all caudal and non-caudal fins*. The factor $C_{friction}{}^{fin}$ is, on the other hand, the shear stress friction created on each side of a fin. The detailed derivation of this coefficient appears in the Electronic Supplement (ES 1). Unlike the body which was likened to a thin, flat rectangular surface of same area for the purpose of friction coefficient calculation (i.e., the K/Re^{α} factor in eqn.3), a non-caudal fin is regarded instead as a thin and two-sided right triangle of base (or "root chord") FC and height

(or "span") FS. The distinction is necessary since the shear stress exerted on a rectangle in the direction of the flow is the same over its width, in contrast to that of a triangle in which both chord and shear stress decreases span-wise from (fin) root to tip. Covering each side of a fin with long (chordwise) and narrow (spanwise) rectangular strips of known shear stress (Fig. ES.1), the friction factor comes out as follows for *each non-caudal fin*

$$C_{friction}^{\ non-caudal-fin} = \left(\frac{(FS)^{2-\alpha}}{SA}\right) \cdot 2 \cdot \frac{K}{(u/\nu)^{\alpha}} \left(\frac{FC}{FS}\right)^{1-\alpha} \left(\frac{1}{2-\alpha}\right) \qquad \text{eqn. A.2}$$

As with the body, the friction drag coefficient of each strip is parameterized by our proxy $C_{friction} = K/Re^{\alpha}$. On the other hand, and being highly swept, caudal fins are instead approximated by two right triangles of differing root chords (FCA and FCB) but of same span (FS), with one triangle inserted into the other in a manner to superpose their span (Figure ES.2). Here FCA is the root chord of the actual swept fin and FCA < FCB by construction. Using strips again to calculate the friction coefficient yields the same equation as A.2, but with the factor $(FC/FS)^{1-\alpha}$ replaced by $(FCA/FS)^{1-\alpha}$.

The parasite drag force of a fin (caudal and non-caudal) is then calculated by multiplying the friction drag coefficient above by the factor $1/2\ \rho_{water}\ u^2\ SA$, per eqn. 2 (*u* being the shark's speed). Note that eqn. A.2 assumes strictly chord-wise flows, thus neglecting cross-flow effects. Note also that with shark bodies and fins being slender, the *parasite* drag formulae discussed in this paper are generally insensitive to angles of attack (AOA), i.e., *when away from stall*. *Induced* drag, on the other hand, *is* sensitive to AOA and specific airfoil profile, but the constraint $W = F_{lift}$ used here allows us to ignore such details as W is known.

Acknowledgments

We would like to thank Yuuki Watanabe and two anonymous referees for their critical comments; they greatly increased the quality of our paper. This project was generously supported by grants from the Australia Pacific Science Foundation, National Geographic's Waitt Foundation Program, the Fisheries Society of the British Isles and the Western Australian Government's NRM program. ACG was supported by Endeavour Research Fellowship. Invaluable field support was provided by the Nyikina-Mangala Rangers. JP thanks G. Bramesfeld for fruitful discussions with regards to estimating the shear stress sustained by triangular flat surfaces

References

Alexander, R. M. (1966). Physical aspects of swimbladder function. *Biological Reviews* **41**, 141-176.

Alexander, R. M. N. (1990). Size, speed and buoyancy adaptations in aquatic animals. *American Zoologist* **30**, 189-196.

Alexander, R. M. N. (2003). Principles of Animal Locomotion. Princeton: Princeton University Press.

Anderson, E. J., McGillis, W. R. and Grosenbaugh, M. A. (2001). The boundary layer of swimming fish. *Journal of Experimental Biology* **204**, 81-102.

Baldridge Jr, H. D. (1970). Sinking factors and average densities of Florida sharks as functions of liver buoyancy. *Copeia*, 744-754.

Ballantyne, J. and Robinson, J. (2010). Freshwater elasmobranchs: a review of their physiology and biochemistry. *Journal of Comparative Physiology B: Biochemical, Systemic, and Environmental Physiology* **180**, 475-493.

Ballantyne, J. S. and Fraser, D. I. (2013). Euryhaline elasmobranchs. In *Fish Physiology: Euryhaline Fishes: Fish Physiology*, vol. 32 eds. S. D. McCormick A. P. Farrell and C. J. Brauner), pp. 125-198: Academic Press.

Blevins, R. D. (1992). Applied fluid dynamics handbook Malabar, FL: Krieger Publishing Company.

Boisclair, D. and Leggett, W. C. (1989). The importance of activity in bioenergetics models applied to actively foraging fishes. *Canadian Journal of Fisheries and Aquatic Sciences* **46**, 1859-1867.

Bone, Q. (1978). Locomotor muscle. In *Fish physiology*, vol. 7 eds. W. S. Hoar and D. J. Randall), pp. 361-424. New York: Academic Press.

Bone, Q. and Roberts, B. L. (1969). The density of elasmobranchs. *J. Mar. Biol. Assoc. UK* **49**, 913-937.

Carlson, J. K. and Parsons, G. R. (1999). Seasonal differences in routine oxygen consumption rates of the bonnethead shark. *Journal of Fish Biology* **55**, 876-879.

Castro-Santos, T. (2006). Modeling the effect of varying swim speeds on fish passage through velocity barriers. *Transactions of the American Fisheries Society* **135**, 1230-1237.

Compagno, L. J. V. (2001). Sharks of the world: an annotated and illustrated catalogue of shark species known to date: FAO.

Corner, E., Denton, E. and Forster, G. (1969). On the buoyancy of some deep-sea sharks. *Proceedings of the Royal Society B: Biological Sciences* **171**, 415-429.

Davenport, J. (1999). Swimbladder volume and body density in an armoured benthic fish, the streaked gurnard.r *Journal of Fish Biology* **55**, 527-534.

Dole, C. E. (1981). Flight Theory and Aerodynamics. New York: John Wiley & Sons.

Fish, F. E. and Shannahan, L. D. (2000). The role of the pectoral fins in body trim of sharks. *Journal of Fish Biology* **56**, 1062-1073.

Ghalambor, C. K., Walker, J. A. and Reznick, D. N. (2003). Multi-trait selection, adaptation, and constraints on the evolution of burst swimming performance. *Integrative and Comparative Biology* **43**, 431-438.

Gleiss, A. C., Jorgensen, S. J., Liebsch, N., Sala, J. E., Norman, B., Hays, G. C., Quintana, F., Grundy, E., Campagna, C. and Trites, A. W. (2011a). Convergent evolution in locomotory patterns of flying and swimming animals. *Nature Communications* **2**, 352.

Gleiss, A. C., Norman, B. and Wilson, R. P. (2011b). Moved by that sinking feeling: variable diving geometry underlies movement strategies in whale sharks. *Functional Ecology* **25**, 595–607.

Greek-Walker, M. and Pull, G. (1975). A survey of red and white muscle in marine fish. *Journal of Fish Biology* **7**, 295-300.

Hainsworth, F. R. (1988). Induced drag savings from ground effect and formation flight in brown pelicans. *Journal of Experimental Biology* **135**, 431-444.

Hussey, N. E., Brush, J., McCarthy, I. D. and Fisk, A. T. (2010). [delta]15N and [delta]13C diet-tissue discrimination factors for large sharks under semi-controlled conditions. *Comparative Biochemistry and Physiology - Part A: Molecular & Integrative Physiology* **155**, 445-453.

Lee, C. E. and Bell, M. A. (1999). Causes and consequences of recent freshwater invasions by saltwater animals. *Trends in Ecology & Evolution* **14**, 284-288.

Long, J. A. (1995). The rise of fishes: 500 million years of evolution: Johns Hopkins University Press Baltimore.

Lowe, C. G. (2001). Metabolic rates of juvenile scalloped hammerhead sharks (Sphyrna lewini). *Marine Biology* **139**, 447-453.

Malins, D. C. and Barone, A. (1970). Glyceryl ether metabolism: regulation of buoyancy in dogfish *Squalus acanthias*. *Science* **167**, 79-80.

Martin, R. A. (2005). Conservation of freshwater and euryhaline elasmobranchs: a review. *Journal of the Marine Biological Association of the United Kingdom* **85**, 1049-1073.

Meloni, C. J., Cech Jr, J. J., Katzman, S. M. and Gatten Jr, R. (2002). Effect of brackish salinities on oxygen consumption of bat rays (Myliobatis californica). *Copeia* **2002**, 462-465.

Oeffner, J. and Lauder, G. V. (2012). The hydrodynamic function of shark skin and two biomimetic applications. *The Journal of experimental biology* **215**, 785-795.

Pelster, B. (2009). Buoyancy Control in Aquatic Vertebrates. *Cardio-Respiratory Control in Vertebrates*, 65-98.

Pillans, R. D. and Franklin, C. E. (2004). Plasma osmolyte concentrations and rectal gland mass of bull sharks *Carcharhinus leucas*, captured along a salinity gradient. *Comparative Biochemistry and Physiology Part A: Molecular & Integrative Physiology* **138**, 363-371.

Pope, A. (1951). Basic Wing and Airfoil Theory. New York: reprinted by Dover Publications.

Priede, I. G., Froese, R., Bailey, D. M., Bergstad, O. A., Collins, M. A., Dyb, J. E., Henriques, C., Jones, E. G. and King, N. (2006). The absence of sharks from abyssal regions of the world's oceans. *Proceedings of the Royal Society B: Biological Sciences* **273**, 1435-1441.

R Development Core Team. (2010). R: A language and environment for statistical computing. Vienna, Austria: R Foundation for Statistical Computing.

Shelton, R. M., Thornycroft, P. J. M. and Lauder, G. V. (2014). Undulatory locomotion of flexible foils as biomimetic models for understanding fish propulsion. *The Journal of experimental biology* **217**, 2110-2120.

Thorburn, D. C. (2006). Biology, ecology and trophic interactions of elasmobranchs and other fishes in riverine waters of Northern Australia., vol. Ph.D., pp. 135. Murdoch: Murdoch University.

Thorson, T. B. (1962). Partitioning of body fluids in the Lake Nicaragua shark and three marine sharks. *Science* **138**, 688-690.

Vermeij, G. J. and Dudley, R. (2000). Why are there so few evolutionary transitions between aquatic and terrestrial ecosystems? *Biological Journal of the Linnean Society* **70**, 541-553.

Videler, J. and Nolet, B. (1990). Costs of swimming measured at optimum speed: scale effects, differences between swimming styles, taxonomic groups and submerged and surface swimming. *Comparative Biochemistry and Physiology Part A: Physiology* **97**, 91-99.

Walker, J., Ghalambor, C., Griset, O., McKenney, D. and Reznick, D. (2005). Do faster starts increase the probability of evading predators? *Functional Ecology* **19**, 808-815.

Ware, D. M. (1978). Bioenergetics of pelagic fish - theoretical changes in swimming speed and ration with body size. *Journal of the Fisheries Research Board of Canada* **35**, 220-228.

Watanabe, Y. Y., Lydersen, C., Fisk, A. T. and Kovacs, K. M. (2012). The slowest fish: Swim speed and tail-beat frequency of Greenland sharks. *Journal of Experimental Marine Biology and Ecology* **426**, 5-11.

Webb, P. (1971a). The swimming energetics of trout II. Oxygen consumption and swimming efficiency. *Journal of Experimental Biology* **55**, 521-540.

Webb, P. W. (1971b). The swimming energetics of trout I. Thrust and power output at cruising speeds. *Journal of Experimental Biology* **55**, 489-520.

Webb, P. W. (1988). Simple Physical Principles and Vertebrate Aquatic Locomotion. *American Zoologist* **28**, 709-725.

Weihs, D. (1973). Optimal fish cruising speed. *Nature* **245**, 48 - 50.

Weitkamp, L. A. (2008). Buoyancy regulation by hatchery and wild coho salmon during the transition from freshwater to marine environments. *Transactions of the American Fisheries Society* **137**, 860-868.

Wetherbee, B. M. and Nichols, P. D. (2000). Lipid composition of the liver oil of deep-sea sharks from the Chatham Rise, New Zealand. *Comparative Biochemistry and Physiology Part B: Biochemistry and Molecular Biology* **125**, 511-521.

Wilga, C. and Lauder, G. (2002). Function of the heterocercal tail in sharks: quantitative wake dynamics during steady horizontal swimming and vertical maneuvering. *Journal of Experimental Biology* **205**, 2365-2374.

Zuur, A. F., Ieno, E. N. and Smith, G. M. (2007). Analysing ecological data: Springer New York.

Table 1 Hypothetical morphological scenarios that were modelled in response to changing salinity. Scenario 0 represents the Null Model of the morphological characters for a 1.25 m bull shark in marine waters.

	Scenario 0 Marine	**Scenario 1** No compensation	**Scenario 2** Increasing Liver Size	**Scenario 3** Decreasing Liver Density	**Scenario 4** Increasing Liver Size + Decreasing Liver Density
Mass (kg)	14.5	14.5	18.3	14.5	18.3
Water Density (kg m^{-3})	1026	996	996	996	996
Lean Tissue Density (kg m^{-3})	1076	1076	1076	1076	1076
Liver Tissue Density (kg m^{-3})	964	964	964	920	920
Lean Tissue Volume (m^3)	0.0118	0.0118	0.0118	0.0118	0.0118
Liver Tissue Volume (m^3)	0.0020	0.0020	0.0045	0.0021	0.0045
Surface Area of body (m^2)	0.59	0.59	0.66	0.59	0. 66
Fineness $\left(\frac{t}{SL}\right)$	0.212	0.212	0.234	0.211	0.234
Projected Frontal Area (m^2)	0.035	0.035	0.045	0.035	0.045
Submerged Weight (N)	4.40	8.44	7.26	7.47	4.44

883 **Table 2 Details of all sawfish and bull sharks that were weighed in air and while**
884 **submerged.**
885
886

	TL (mm)	Mass (g)	W_{sub} (N)	Buoyancy Ratio (%)	V (ml)	P_{Shark} (kg m^{-3})
C. leucas	862	4175	2.50	6.11	3936	1060.8
C. leucas	824	3390	2.35	7.08	3163	1071.9
C. leucas	851	4145	2.60	6.39	3896	1064.0
C. leucas	950	4815	2.89	6.13	4538	1061.0
C. leucas	840	3765	2.40	6.51	3534	1065.3
P. pristis	1224	4600	2.74	6.07	4338	1060.3
P. pristis	1018	2365	1.47	6.34	2224	1063.4
P. pristis	1140	3780	2.48	6.69	3541	1067.4
P. pristis	1151	3660	2.26	6.28	3444	1062.8
P. pristis	1090	3130	1.91	6.23	2947	1062.2
P. pristis	1082	2890	1.81	6.40	2716	1064.1
P. pristis	1025	3015	1.81	6.14	2841	1061.1
P. pristis	1119	3060	2.01	6.70	2866	1067.5
P. pristis	1021	2170	1.32	6.22	2043	1062.1
P. pristis	1207	4230	2.75	6.62	3966	1066.6
P. pristis	1079	2765	1.77	6.51	2595	1065.4
P. pristis	1040	2760	1.96	7.25	2570	1073.8
P. pristis	1104	2895	1.91	6.74	2711	1067.9
P. pristis	1025	2215	1.47	6.77	2073	1068.3
P. pristis	912	1530	1.03	6.86	1431	1069.4
P. pristis	1172	4000	2.50	6.38	3760	1063.8
P. pristis	1120	3600	2.11	5.97	3399	1059.3

Table 3 Details of the sawfish (n=2) and bull sharks (n=3) that were available for full necropsies.

	Carcharhinus leucas				*Pristis pristis*		
	1	***2***	***3***	**Mean**	***1***	***2***	**Mean**
Total length (mm)	862	824	851	*846 ± 20*	1146	1130	*1138 ± 11*
Mass (g)	4175	3390	4145	*3903 ± 445*	4000	3600	*3800 ± 283*
W_{sub} (N)	2.50	2.35	2.60	*253 ± 13*	2.50	2.07	*235 ± 28*
Body Volume (ml)	4429	3634	4410	*4158 ± 454*	4255	3813	*4034 ± 312*
% Mass / Submerged Weight	6.11	7.08	6.39	*6.53 ± 0.50*	6.38	5.97	*6.17 ± 0.28*
Mass excluding liver (g)	3860	3150	3750	*3587 ± 382*	3770	3360	*3565 ± 290*
Submerged Weight excluding liver (g)	280	225	260	*255 ± 28*	255	215	*235 ± 28*
Liver Mass (g)	410	226	289	*308 ± 93*	230	240	*235 ± 7*
Liver Volume (ml)	450	235	320	*335 ± 108*	234	245	*240 ± 8*
Body Volume excluding Liver (ml)	3594	2937	3504	*3345 ± 356*	4021	3579	*3800 ± 312*
Body Density (kg m^{-3})	1061	1072	1064	*1066 ± 6*	1064	1059	*1060 ± 3*
Body Density excluding liver (kg m^{-3})	1074	1073	1070	*1072 ± 2*	1068	1064	*1066 ± 3*
% Liver Volume	7.71	6.22	8.88	*7.60 ± 1.33*	5.51	6.15	*5.83 + 0,45*
% Liver Mass	9.81	6.65	6.98	*7.82 ± 1.74*	5.75	6.67	*6.21 ± 0.65*
Liver Density (kg m^{-3})	910	960	904	*920 ± 31*	982	980	*981 ± 2*

Table 4 Model selection criteria for 3 analysis (Fig. 2) comparing morphological data from freshwater elasmobranchs sampled as part of this study and marine forms published in previous papers (Baldridge Jr, 1970; Bone and Roberts, 1969).

	Model	df	logLik	AICc	delta	weight
Mass vs Liver Mass	logLiverMass ~ logMass	4	45.88	-83.4	0	0.433
	logLiverMass ~ logMass + Lifestyle	6	47.21	-82.3	1.14	0.245
	logLiverMass ~ logMass + Lifestyle + Habitat	5	46.179	-81.8	1.6	0.194
	logLiverMass ~ logMass + Habitat	7	48.002	-81	2.44	0.128
Mass vs Wsub	logWsub ~ logMass + Habitat	5	122.817	-233.9	0	0.5
	logWsub ~ logMass + Lifestyle + Habitat + logMass * Lifestyle	6	122.92	-231.7	2.18	0.168
	logWsub ~ logMass + Lifestyle	4	123.057	231.2	2.67	0.131
	logWsub ~ logMass + Habitat*Lifestyle	7	119.679	231.1	2.86	0.12
Liver Density	P_{Liver} ~ Lifestyle + Habitat	6	254.169	-495.6	0	0.865
	P_{Liver} ~ Lifestyle	5	251.078	-491.6	3.96	0.120
	P_{Liver} ~ Habitat	4	247.401	-486.4	9.13	0.009
	P_{Liver} ~ 1	1	245.926	-485.6	9.94	0.006
Lean Tissue Density	$P_{Lean\ Tissue\ Density}$ ~ 1	1	77.389	-148.6	0	0.605
	$P_{Lean\ Tissue\ Density}$ ~ Habitat	4	77.415	-146.5	2.08	0.214
	$P_{Lean\ Tissue\ Density}$ ~ Lifestyle	5	78.033	145.6	3.01	0.135
	$P_{Lean\ Tissue\ Density}$ ~ Lifestyle + Habitat	6	78.059	-143.4	5.16	0.046

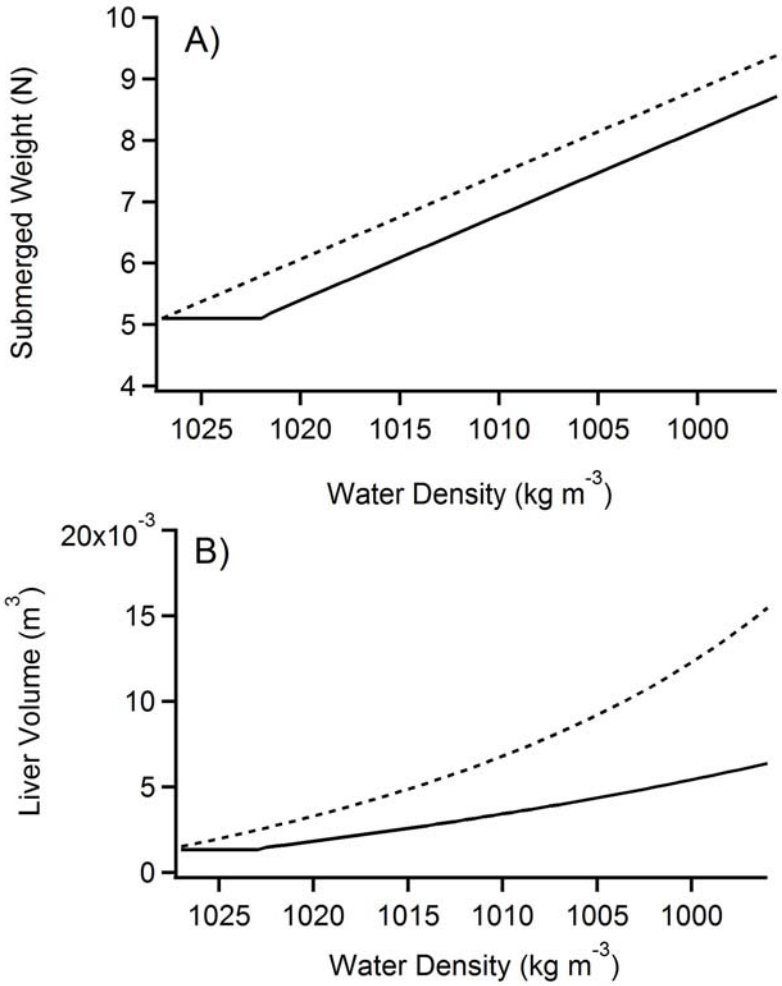

Figure 1 Modelled implications of water density for the buoyancy control of elasmobranchs. Data were modelled based on the equation 1 and parameterised with a hypothetical shark of 15 kg with the same body composition and tissue densities as those observed in Baldridge (Baldridge Jr, 1970). The stippled line indicates the response to changing environmental density if no compensation in liver density occurs. The solid lines represents the same model, assuming that the animal has the ability to reduce its liver density to those encountered in neutrally buoyant deep-sea sharks (~920 kg m^{-3}) representing the lowest liver densities encountered in elasmobranchs. A) Assuming no morphological changes (i.e. constant tissue volumes and densities), submerged weight would increase by ~120% for a shark moving into freshwater. A reduction in liver density to 920 kg m^{-3} would be able to compensate any changes in water density up to ~1025 kg m^{-3}, yet still resulting in submerged weight doubling. B) Negative buoyancy may also be compensated by changes in liver size; in order to maintain the same submerged weight (4.5 N) as in marine waters, our hypothetical shark's liver would have to increase 8-fold in volume (stippled line) and even if liver density would be reduced, liver volume would have to increase 3-4 fold to maintain similar buoyancy as in marine waters. These cases would result in liver size comprising 70% or 35% of whole body volume respectively compared to 11% in marine waters. In all scenarios described, lean tissue density and volume are unchanged.

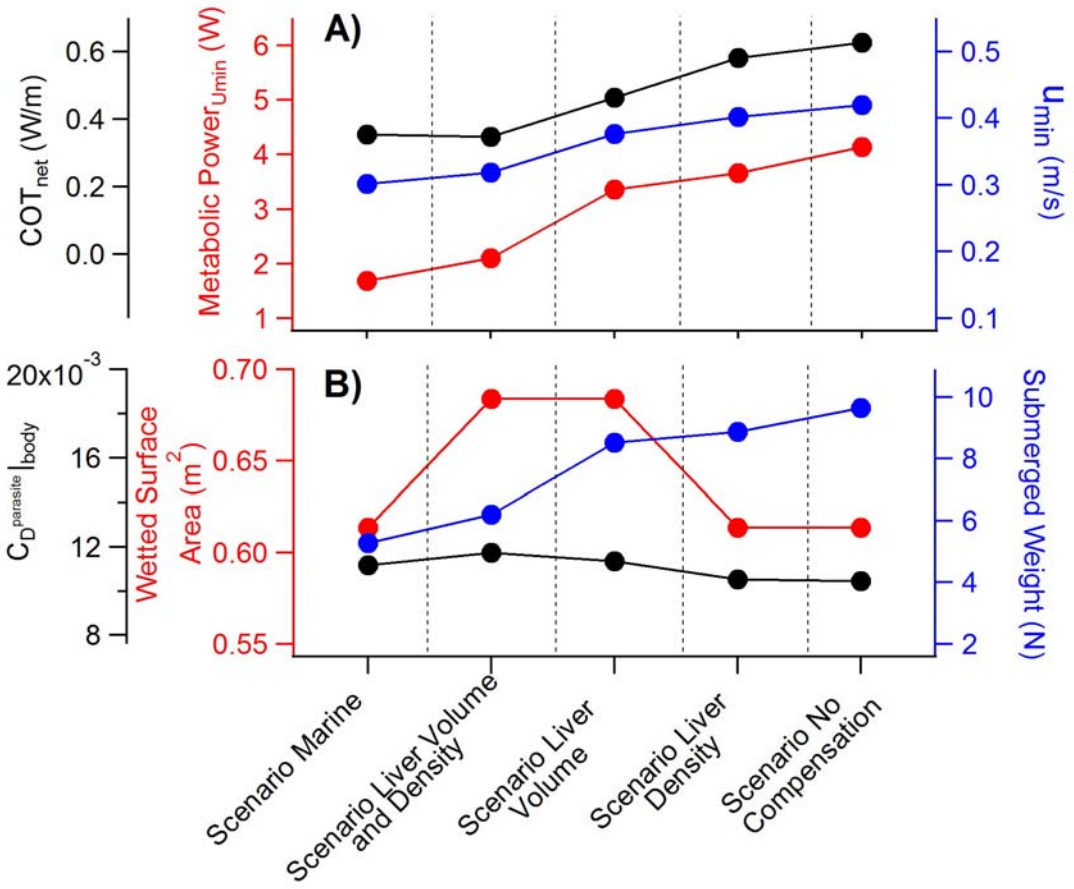

Figure 2 Paramters and results of our modelling excersise (bull shark, 1.2m standard length). A) All scenarios result in increasing costs of locomotion, as a result of increasing u_{min} which increases drag. All hypohtetical scenarios also result in increasing cost of tranbsport, with the exception of the scenario where liver size increases and liver density decreases. B) This pattern is a result of all scenarios being characteristic of increased negative buoyancy, with the lowest increase where both density and size have been altered. Based on our considerations of u_{min}, all potential compensatory strategies result in increased costs. Based on u_{min}, increases in liver size and liver density should be the optimal strategy for compensation. This however, ignores the cost of swimming at faster speeds, which are discussed in Figure 4.

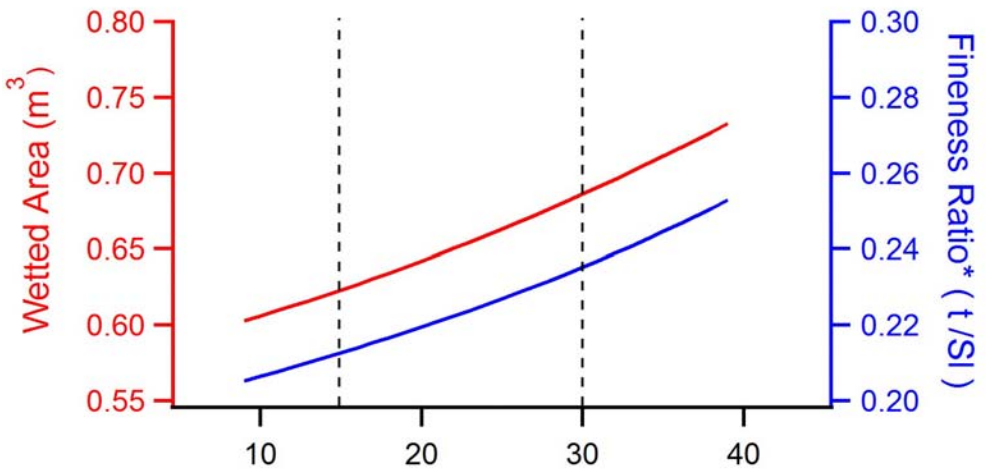

Figure 3 Hydrodynamics of increasing liver size. To gauge the costs associated with faster speeds that may be employed during foraging, here we model the implications of increasing liver sizes on drag. As induced drag responds $1/u^2$, its contribution to total drag at greater speeds will diminish, while parasitedrag will increase u^2. Here we show that increasing liver size results in an increase of two of the primary parameters that contribute to parasite drag. All things being equal, drag is proportional to wetted area (eqn. 3) and our approximation suggests that this parameter will increase by >10% from liver volume of 15% - 30% (dashed vertical lines). The Fineness Ratio is the dominant factor in the calculation of $C_D^{parasite}\big|_{body}$ (eqn. 3). Increasing the fineness ratio by 10% subsequently results in a less streamlined body and a higher drag coefficient proportional to that increase. These data therefore suggest that compensatory mechanisms involving increasing liver size may reduce the costs at low swimming speeds, but will result in significantly increased costs at faster speeds. *Please note that our definition of fineness ratio is the inverse of its typical use. We have chosen to adhere to this format as a result of the formulation in eqn. 3.

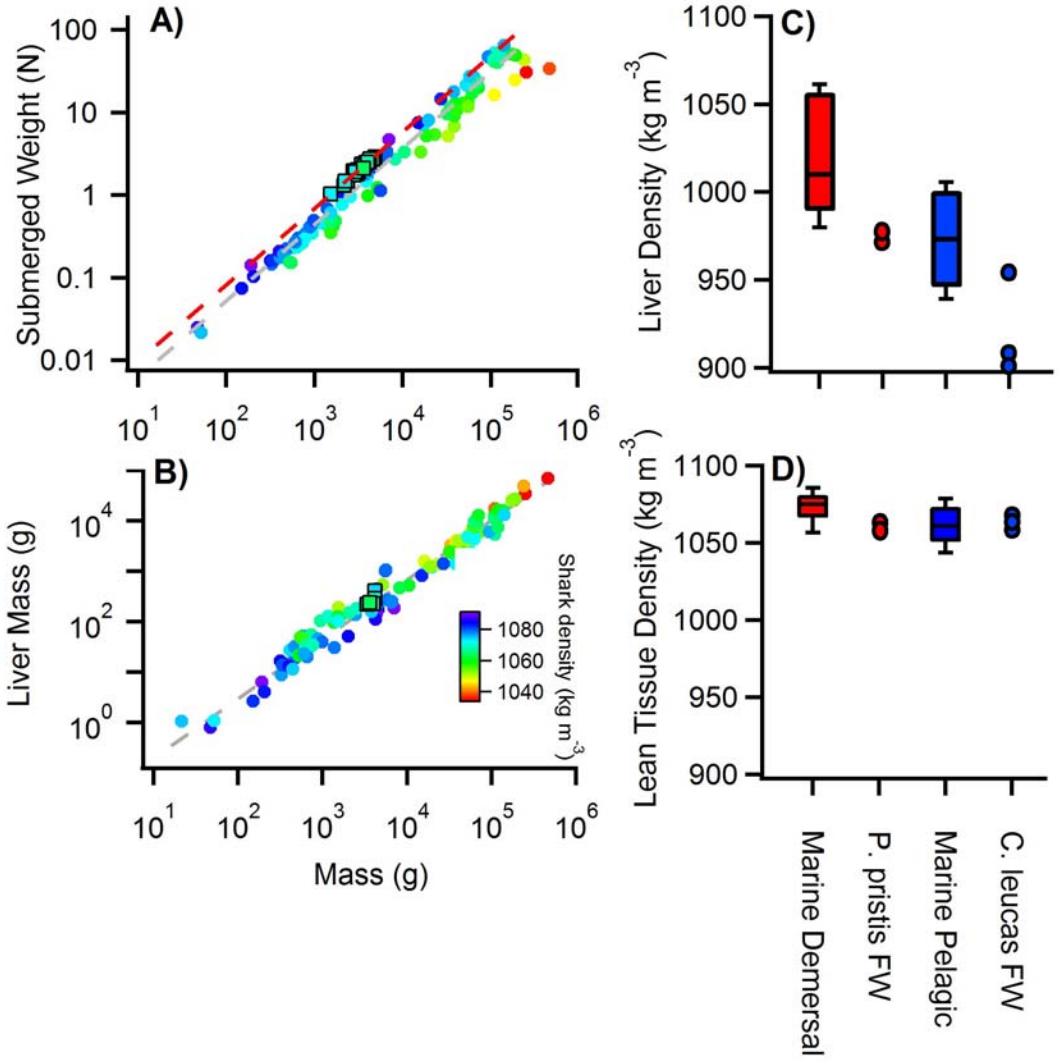

Figure 4 Morphological differences in marine and freshwater elasmobranchs. A) Significant differences were found in the submerged weight between all individuals sampled by Bone and Roberts (1970) and Baldridge Jr (1970) in marine waters (grey stippled line, excluding species that are neutrally buoyant, such as deep-sea sharks and the basking shark, *Cetorhinus maximus*) and *Carcharhinus leucas* (n=5) and *Pristis pristis* (n=20) sampled in freshwater as part of this study (red stippled line). B) No differences in liver size between individuals sampled in marine environments and the 2 sawfish and 3 bull sharks that were available for full necropsy. C) Comparison of liver density in the sharks sampled from marine waters and those from freshwater. The lifestyle of the species has a significant effect on liver density, with demersal individuals having denser livers than those that are pelagic. The two species we sampled in freshwater were close or below the lower 90th percentile for all marine individuals sampled previously suggesting that individuals occupying freshwater may have lower liver densities. D) No major differences in lean tissue density could be detected between either lifestyles or habitat. See Table 4 for the model selection for all three analyses.